Design and Test of an Air-assisted Electrostatic Nozzle

Liangfu Zhou[1,*], Yang Gu[2]
[1]Nanjing Vocational University of Industry Technology, Nanjing, Jiangsu, China
[2]Suzhou Yuanliang Intelligent Equipment Technology Co., Ltd, Suzhou, Jiangsu, China
**Corresponding Author.*

Abstract: In order to solve the problems of easy adsorption of charged droplets at the nozzle and easy attenuation of the charged power in the direction of range, the air-fed electrostatic nozzle was designed by combining airflow-assisted spraying and electrostatic spray technology. Theoretical analysis and experimental methods were used to determine the structure and parameters of the induction electrode and the structure and parameters of the airflow channel. The results of the nozzle performance test showed that when the spray distance was greater than 1.5m, and the electrostatic spray lost its effect. This study provides technical support for the popularization and application of electrostatic nozzles, and provides a reference for the design of large-scale sprayers with this type of nozzle as components.

Keywords: Plant Protection Machine; Droplet; Electrostatic Spray; Airflow; Charge-to-Mass Ratio

1. Introduction

Electrostatic spraying relies on the electrostatic benefit between the charged droplets and the crop target, which greatly increases the amount of pesticide deposition on the plant surface and reduces pesticide drift [1]. A large number of scholars at home and abroad have done a lot of research work on electrostatic spraying, and Jia Weidong et al. [2] used PDPA to study the relationship between charging voltage and spray performance, and applied and tested it on an air curtain boom sprayer [3]. Moon et al. [4] designed an annular inductive electrostatic nozzle, which found that the target region had a large charge current, up to 27 microamperes, by loading a pulse voltage. Ru Yu et al. designed an aeronautical dual-nozzle electrostatic nozzle [5] to analyze the effect of the double-nozzle annular electrode on the space electric field and charging effect. According to the application characteristics of aviation electrostatic nozzles in light aircraft, the design of electrostatic electrodes, nozzle materials, and nozzle processing technology was improved [6]. Law et al. [7-8] were the first to develop the airflow atomization electrostatic sprayer MaxCharge, and then the United States ESS company developed a series of electrostatic sprayers on this basis, and Pascuzzi et al. [9] used their 150RB14 suspended electrostatic sprayer to conduct systematic tests in vineyards. Mamidi et al. [10] designed a knapsack handheld electrostatic sprayer on the basis of optimizing the electrode structure and position, and tested it in potted crops, and its coverage and uniformity were improved by 2-3 times. Durham et al. [11] investigated the effects of induced voltage, operating speed, target height, and spray direction on droplet coverage. Zhao et al. [12] numerically analyzed the specified trajectories of droplets under droplet size, charge-to-mass ratio and spray distance, and concluded that the droplet drift and deposition increased with the increase of load-to-mass ratio, and were greatly affected by the spray distance. Wu et al. [13] studied the characteristics of gas-assisted electrostatic spray on the back of the target, and the electrostatic voltage, spray distance and air velocity all had great effects on the back deposition. In this paper, the relationship between the charging process of droplets, the attenuation of charged droplets and the airflow velocity is analyzed, and the dual-airflow auxiliary electrostatic sprinklers are designed, and the effect of the electrostatic sprinklers is verified by experiments, so as to provide technical support for the application of the nozzle and the design of the implements.

2. The Structure and Principle of the Nozzle

2.1 Main Structure

In order to improve the rapid transport capacity

of charged droplets of the electrostatic nozzle, the air-fed electrostatic nozzle adopts a combination of an airflow auxiliary system and an inductive electrostatic system, and the main structure is shown in Figure 1. The airflow auxiliary system mainly includes a hair dryer, a motor (motor speed 10000r/min) and an impeller, and the induction electrostatic system includes a hollow cone mist nozzle, an induction electrode, an air flow channel and a fixed pipe. Among them, the induction electrode is built into the electrode base made of high insulating epoxy resin, and the output voltage of the selected high-voltage electrostatic generator is 10000-20000V, the power is less than 4W, and the input voltage is 12V.

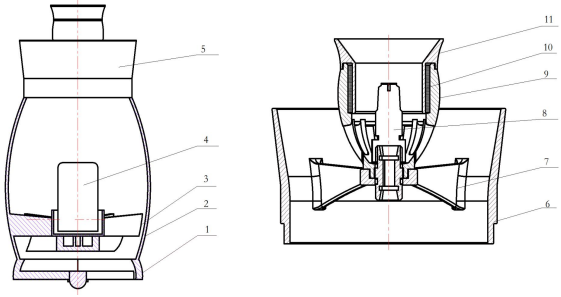

a. Air Electrostatic Nozzle b. Electrostatic Head Assembly
1. Hair Dryer Back Cover 2. Hair Dryer Body 3.Impeller 4.Motor 5.Electrostatic Head Assembly 6.Outer Front Deflector 7.Nozzle Support Seat 8.Nozzle 9.Inner Air Channel 10.Electrode 11.Inner Front Shroud
Figure 1. Structure of Air Electrostatic Nozzle

2.2 How It Works

Driven by the DC motor, the impeller generates an air flow at a speed of 10,000r/min, which is divided into two by the inner cylinder, one of which directly flows out of the outer front cover to transport fog droplets. The other part of the airflow flows into the electrostatic head assembly and flows out from the inner front deflector to prevent the charged droplets from adsorbing on the nozzle. Under the action of high-voltage power supply (liquid path grounding), a high-voltage electric field is formed between the electrode and the fog flow, and when the atomized fog droplets enter the electric field area, they will be induced into a charge opposite to the electrode, and the charged fog droplets are quickly transported to the crop target under the action of the air flow in the inner flow channel.

3 Key Structures and Parameters

3.1 Electrostatic Head Assembly

The electrostatic head assembly comprises a pipe joint, an atomizing nozzle and a nozzle cover, and the top of the air flow channel is correspondingly provided with a nozzle mount, and the pipe joint is arranged through the mounting seat and the top of the air flow channel. The atomizing nozzle is correspondingly arranged in the air flow channel, and the atomizing nozzle is correspondingly installed at the bottom of the pipe joint. The annular electrode is embedded in the air flow channel and the front shroud, and the electrode ring can be connected with one end of the power supply through a connecting wire when used, and the other end of the power supply is grounded. Wherein the air flow channel is threaded with the mounting seat. The top of the atomizing nozzle is connected with the bottom of the pipe joint in a threaded manner, and the inner ring of the mounting seat can be installed on the pipe joint corresponding to the clamping, and the interference fit between the pipe joint and the mounting seat. The front shroud is installed at the bottom of the airflow channel by means of interference fit clamping, and the lower part of the inner hole expands downward in the shape of a bell to facilitate airflow diffusion. The structure of electrostatic nozzle assembly is shown in Figure 2.

In order to ensure the use effect of the electrostatic sprinkler, the relevant parameters of the electrostatic sprinkler are optimally designed. That is, the thickness of the electrode ring 5 is preferably 2-3mm, and can be set to 3mm when it is actually manufactured. The induced voltage of described electrode ring 5 is preferably 8-10KV, and can be set to 10KV when actually working. The angle of inclination at the bottom of the inner bore of the inner front shroud α preferably set to 52°. The relationship between the installation position of described atomizing nozzle and electrode ring 5 is D=2~2.4L; wherein D is the inner ring diameter of electrode ring, and L is the vertical distance L between atomizing nozzle bottom and electrode ring bottom.

a. Structure of Electrostatic Nozzle b. Photos of Electrostatic Nozzle

1. Pipe Joint 2. Mounts 3.Nozzles 4.Air Runners 5.Annular Electrodes 6.Inner Front Shrouds

Figure 2. Electrostatic Nozzle Assembly

3.2 Airway Design

In order to ensure the charging effect of the droplets, it is not desirable to reduce the electric field strength and the charge of the droplets, so only by increasing the drag force of the airflow can the droplets be transported out of the strong electric field area and the droplets do not gather at the nozzle electrode. In order to avoid the attenuation of the charge of the droplets caused by the airflow velocity gradient after the droplets are separated from the strong field area, the larger the theoretical velocity of the designed airflow, the more advantageous it is. The 3D drawing of wind turbine is shown in Figure 3.

Therefore, the selected motor parameters are 48V, 10000 rpm, the impeller diameter is 130mm, the diameter of the hair dryer outlet is 114mm, and the inner front shroud is designed with 12 profiled air intake grids, and the size of the air intake grid is 5×20mm.

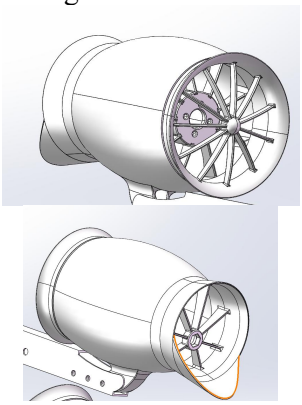

a. Back view b. Front view

Figure 3. 3D drawing of Wind Turbine Components

4. Performance Test

4.1 Airflow Field Characteristics

4.1.1 Axial velocity attenuation characteristics

Under the impeller speed of 10000r/min, a tape measure and anemometer are used, and the test line is set every 0.2m within the range of the nozzle airflow axial direction of 3m, and the anemometer is sampled in the axis direction to read the airflow velocity values at different distances, and the curve is drawn by Excel software as shown in Figure 4. As can be seen from the figure, the air flow nozzle outlet decays rapidly after ejection, and when the distance is greater than 1.6m, the effective airflow velocity is less than 2m/s, and the ability to transport droplets is lost.

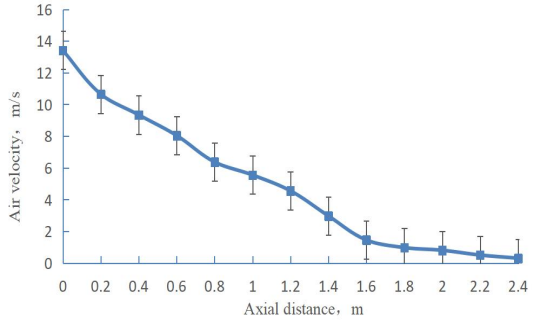

Figure 4. Axial Attenuation of Airflow

4.1.2 Turbulence characteristics

Turbulence intensity is one of the important characteristic quantities to describe the characteristics of air flow field, which describes the degree of variation of wind speed with time and space, and reflects the relative intensity of fluctuating wind speed. In this study, the Kestrel 4500 anemometer was used to test the transient velocity change of the airflow at the outlet of the sprayer within 1 min at 10000 r/min, and the curve was plotted by Excel software, as shown in Figure 5. As can be seen from Figure 5, the airflow at the outlet of the nozzle has turbulent properties, and its airflow velocity fluctuates within 12~14m/s, and its turbulence intensity is 5.6% according to the turbulence intensity calculation formula,

which can effectively promote the flipping of the target and facilitate the deposition of charged droplets on the back.

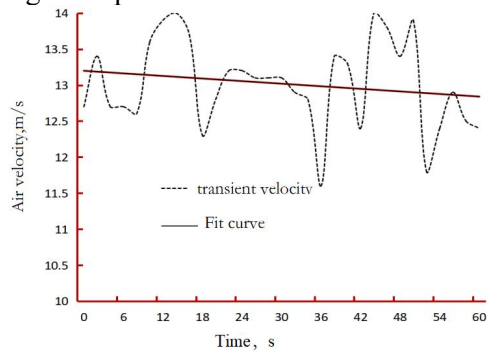

Figure 5. Turbulence Characteristics of Airflow

4.2 Electrostatic Effect Test

4.2.1 Charge-to-mass ratio test

The Faraday cylinder method is used to test the charge, that is, the airflow auxiliary electrostatic nozzle is installed on the central axis 200 mm away from the inlet of the Faraday cylinder, and the Faraday cylinder with an inner diameter of 550 mm collects all the droplets. A Keysight 34410A digital multimeter (100 microamperes, 61/2 digit readings) was used to measure the charged current I of all droplets, and the quality of the fog flow from the Faraday cylinder within 1 minute was recorded. The load-to-mass ratios of 0.2, 0.6, 0.8, 1.0, 1.4 and 1.8 m were mainly tested at the spray flow rate of 700ml/mim, the induced voltage of 10KV and the outlet airflow velocity of 13m/s, and the test results are shown in Figure 6.

As can be seen from Figure 6, the load-to-mass ratio is about 0.95 mC/kg at 0.2 m away from the nozzle outlet, and the charge-to-mass ratio gradually decays along the range direction, and when the spray distance is greater than 1 m, the charge-to-mass ratio is less than 0.4 mC/kg. Therefore, when formulating field operation parameters, it is necessary to select the spray distance according to the operation requirements, and it is recommended that the spray distance should be within 0.8m to ensure the charging effect.

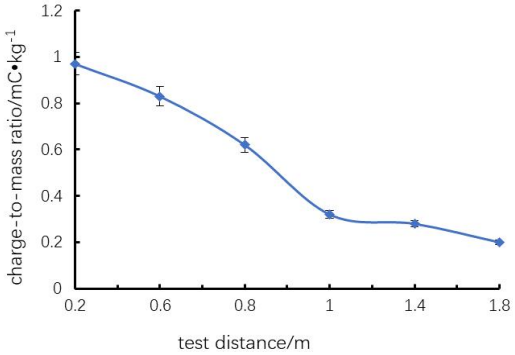

Figure 6. Charge-To-Mass Ratio Attenuation Law

4.2.2 Deposition test

The test collection points are arranged according to Figure 7, wherein the collection distance is 3m, the collection spacing is 0.5m, the collection height is 1m, each collection distance is arranged A, B, C three collection points, each collection point is arranged with a size of 26×76mm 2 pieces of water-sensitive paper to detect the positive and negative fog droplet deposition, and the average value of 3 points at each distance is used as the test result. The nozzle sprays at a certain speed at a distance of 1.1 m from the ground, passes through the collection area under two working conditions, electrostatic and non-electrostatic, collects the paper card in a ziplock bag after drying on the water-sensitive paper, collects the droplet coverage image with a microscopic camera on the same day, and uses the droplet image processing system to measure the droplet distribution on the paper card. The data are recorded in Table 1, and it can be seen from Table 1 that the coverage density of the front droplets is slightly smaller than that of non-electrostatic spray. When the electrostatic spray is less than 1.0 m, the coverage density of the reverse droplet of electrostatic spray is more than 10% higher than that of non-electrostatic spray, and it can still be increased by more than 7% within 1.5m, and when the distance is greater than 2m, the electrostatic spray will lose its effect.

Table 1. Comparison of Electrostatic Spray Effects at Different Distances (Droplets per Unit Area/pc•cm^{-2})

Test distance	0.5 m		1 m		1.5 m		2 m		2.5 m		3 m	
	front	back	front	back	front	back	front	back	front	back	front	back
electrostatic	168	120	160	119	113	66	75	35	45	20	22	10
non-electrostatic	170	85	165	105	114	61	73	34	44	21	25	9
Relative increase/%	-1.19	29.17	-3.13	11.76	-0.88	7.58	2.67	2.86	2.22	-5.00	-13.64	10.00

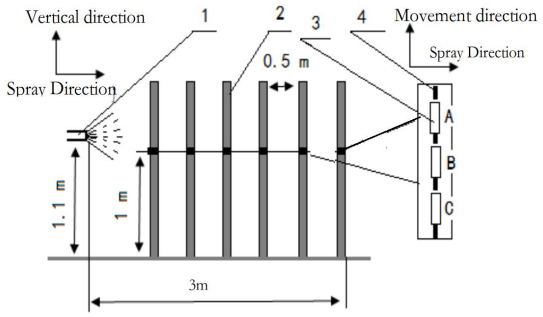

1. Nozzle 2. Collection Rack 3. Water-Sensitive Paper 4. Nylon Rope
Figure 7. Schematic Diagram of Distribution Test

5. Conclusion

In order to improve the deposition efficiency of the droplets on the back of the canopy target, an air-assisted electrostatic nozzle was designed, and the charge-to-mass ratio at the outlet of the nozzle reached 0.951mC/kg and the turbulence intensity of the airflow was greater than 5% under the condition of induced voltage of 10KV and the airflow velocity of the nozzle outlet was 13m/s. When the spray distance is greater than 1.5m, the airflow velocity and load-to-mass ratio decay to 2m/s and 0.35mC/kg, respectively. The results of the spray deposition test also showed that when the spray distance was greater than 1.5m, the electrostatic spray lost its effect. This study provides technical support for the popularization and application of electrostatic nozzles, and provides a reference for the design of large-scale sprayers with this type of nozzle as components.

Acknowledgements

This project is supported by independent innovation of agricultural science and technology of Jiangsu Province (Grant No. CX(22)3103); Jiangsu Province Precision Manufacturing Engineering and Technology Research Center.

References

[1] Law, S. E. Agricultural electrostatic spray application: a review of significant research and development during the 20th century, 2001. J. Electrost. 51-52.
[2] Jia Weidong, Li Pingping, Qiu Baijing, et al. Experimental study on particle size and velocity distribution of agricultural charged spray droplets. Transactions of the CSAE, 2008, 24(2):17-21
[3] Jia Weidong, Hu Huachao, Chen Long, et al. Atomization and droplet deposition performance test of air curtain electrostatic spray rod spray nozzle. Transactions of the CSAE, 2015, 31(7):53-59.
[4] Moon J, Lee D, Kang T, et al. A capacitive type of electrostatic spraying nozzle. Journal of Electrostatics, 2003, 57(2): 363－379.
[5] Ru Yu, Zheng J, Zhou H, et al. Design and test of aviation double-nozzle electrostatic nozzle. Transactions of the CSAM, 2007, 38(5):58-61.
[6] Ru Yu, Jin Lan, Jia Zhicheng, et al. Design and test of unmanned aerial vehicle electrostatic spray system. Transactions of the CSAE, 2015, 31(8):42-47.
[7] Law, S.E., 1977. Electrostatic spray nozzle system. U. S. Patent No. 4,004,733. U. S. Patent Office, Washington, D. C.
[8] Law, S. E., 1978. Embedded-electrode electrostatic-induction spray-charging nozzle: theoretical and engineering design. Trans. ASAE 21 (6), 1096-1104.
[9] Pascuzzi S, Cerruto E. Spray deposition in “tendone” vineyards when using a pneumatic electrostatic sprayer. Crop Protection, 2015, 68(3): 1-11.
[10] Mamidi V R, Ghanshyam C, Kumar P M, et al. Electrostatic hand pressure knapsack spray system with enhanced performance for small scale farms. Journal of Electrostatics, 2013, 71(4): 785-790.
[11] Durham K. Effects of conventional and reduced-volume, charged-spray application techniques on dislodgeable foliar residue of captan on Strawberries. Agric. FoodChem. 1991(39): 1646-1651.
[12] Zhao S. Castle G.S.P, Adamiak K. Factors affecting deposition in electrostatic pesticide spraying. Journal of Electrostatics. 2008(66):594-601.
[13] Wu Chundu, Shi Yanan, Zhang Bo, et al. Characteristics of dorsal deposition of gas-assisted electrostatic spray targets. Drainage and Irrigation Machinery. 2009, 27 (04):242-245.

